Materials Science in Semiconductor Processing 17 (2014) 129–133

Contents lists available at ScienceDirect

Materials Science in Semiconductor Processing

journal homepage: www.elsevier.com/locate/mssp

# Synthesis of NiO nanospheres with ultrasonic method for supercapacitors

Wanhong Sun [a,*], Lihua Chen [a], Shujuan Meng [b], Yanbin Wang [b], Hailing Li [a], Yongchao Han [b], Na Wei [b]

[a] Experiment Center of Northwest University for Nationalities, Lanzhou 730030, China
[b] College of Chemical Engineering, Northwest University for Nationalities, Lanzhou 730030, China

ARTICLE INFO

Available online 6 October 2013

*Keywords:*
NiO
Ultrasound techniques
Nanoparticle

ABSTRACT

NiO nanospheres have been synthesized by using magnetic stirring and ultrasound methods. The structure and morphology of synthesized samples were characterized by X-ray diffraction, scanning electron microscopy and high resolution transmission electron microscopy. The results show the NiO nanospheres prepared by the ultrasonic method are far less than that prepared by the stirring method. Moreover, in the presence of surfactant, the average diameter of NiO nanospheres prepared by the ultrasonic method is only 1–3 nm. The capacitance of NiO electrodes was investigated with cyclic voltammetry. The NiO prepared by the ultrasonic method exhibited higher specific capacitance of $\sim$260 F g$^{-1}$ at 1 A g$^{-1}$ current density.

© 2013 Elsevier Ltd. All rights reserved.

## 1. Introduction

Recently, nickel oxides (NiO) have been widely investigated due to their potential applications in electrochromic films, sensor, electrochemical capacitors, photocatalysts, batteries, photoelectrodes, etc. [1–5]. Nanostructured NiO with wide band gap (3.6–4.0 eV) is believed to have better properties than those of their bulk materials. Because of these facts, many research scientists are working hard to develop various methods for the synthesis of high quality nanostructured materials. Several approaches have been used to prepare NiO nanostructures, including spray pyrolysis [6], chemical vapor deposition [7], sol–gel method [8] and precipitation method [9]. However, most of these methods are time-consuming, complicated and expensive, or require a relatively high temperature [10]. Therefore, the development of a simple and fast synthetic route that can generate a high-quality NiO material remained an important topic of investigation.

Some of the promising technique may be the use of ultrasound and microwave as alternative energy sources for the preparation in organic synthesis, catalytic reactions, and environmental and engineering sciences [11,12]. Ultrasound technique can produce hot spots during the rarefaction phase of sound waves. It has been estimated that these hot spots have temperatures about 5000 K with cooling rates above $1\times10^{10}$ K s$^{-1}$, and pressures of the order of 100 MPa. The kinetic energy released under these conditions and promoted both physical effects and chemical reactions that can directly influence the particle size and morphology of prepared products [13,14].

In this study, NiO nanospheres having good dispersibility were prepared by ultrasound technique. The effect of surfactant on the electrochemical properties of NiO nanospheres was also paid attention. The morphology was observed by scanning electron microscopy (SEM) and transmission electron microscopy (TEM), and the crystal geometry was characterized by X-ray diffractometer.

## 2. Experiment

### 2.1. Sample preparation

Nickel sulfate, sodium dodecyl benzene sulfonate (SDBS) and potassium hydroxide at analytical reagent grade were

* Corresponding author. Tel.: +86 931 4512923.
*E-mail address:* sunwh2004@126.com (W. Sun).

1369-8001/$ - see front matter © 2013 Elsevier Ltd. All rights reserved.
http://dx.doi.org/10.1016/j.mssp.2013.09.002

obtained from commercial suppliers and used as received. The NiO nanospheres were synthesized with and without ultrasound technique as follows. Forty milliliters of 0.02 mol/L KOH aqueous solution were slowly dropped into 50 mL of 0.02 mol/L nickel sulfate solution under an ultrasonic water bath at power 80 W or in the heating magnetic stirring for 6 h. The solution was removed from the sonicator or magnetic stirrer and kept for 24 h at room temperature without stirring. The colloidal precipitate was collected by centrifugation, washed with water and ethanol several times, and dried at 50 °C under vacuum for 24 h. The obtained product was sufficiently ground and then calcined at 350 °C for 2 h. The same procedure was repeated under an ultrasonic water bath at power 80 W except that 3.5 mg of sodium dodecyl benzene sulfonate was added into the above nickel sulfate solution. The samples prepared under various methods are denoted as NiO-1 (magnetic stirring), NiO-2 (ultrasound) and NiO-3 (ultrasound with SDBS surfactant).

### 2.2. Characterization

X-ray diffration studies were performed by using D/max-2400 diffraction X-ray diffractometer (Rigaku) with CuKa as a radiation source. Scanning electron microscope (SEM, Hitachi, Japan, JEOL, JSM-6330F) was used to observe the morphologies of composite. Prior to the examination, the specimens were coated with a very thin layer of gold. Transmission electron microscopy (TEM) was performed with a TECNAI $G^2$ model transmission electron microscope at 100 kV accelerated voltage and the observations were carried out after retrieving the slices onto Cu grids.

### 2.3. Electrochemical tests

The working electrodes were prepared according to the following steps. The typical mass load of the electrode materials is 10 mg 75 wt% of active materials was mixed with 7.5 wt% of acetylene black and 7.5 wt% of conducting graphite in an agate mortar until a homogeneous black powder was obtained. To this mixture, 10 wt% polytetrafluoroethylene was added with a few drops of ethanol. The resulting paste was pressed at 10 MPa to a foam nickel grid that served as a current collector. Each electrode contained about 5 mg of electroactive material and had a geometric surface area of about 1 $cm^2$. A typical three-electrode experimental cell equipped with a working electrode, a platinum foil counter electrode, and a saturated calomel reference electrode (SCE) was used for measuring the electrochemical properties of the working electrode and its performance was a Faradic electrochemical capacitances (ECs). All electrochemical measurements were carried out on CHI660B electrochemical working station in 6 M KOH aqueous solution as electrolyte at 25 °C.

## 3. Results and discussion

XRD diffraction data for the polycrystalline materials provided information about the phase composition and the degree of crystallinity of the particle nanostructure. The mean crystallite dimension, or size, of the coherent

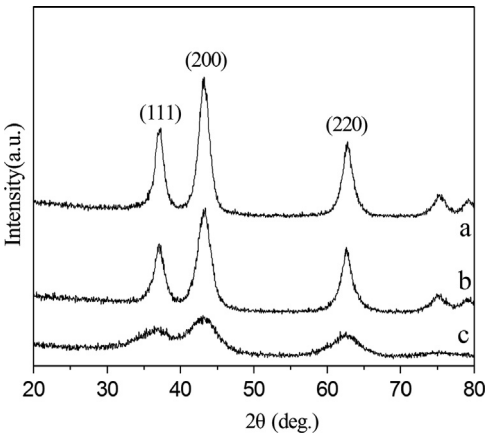


**Fig. 1.** XRD for prepared NiO-1 (a), NiO-2 (b) and NiO-3 (c).

crystalline domain and the lattice imperfections can be estimated from peak broadening [15]. Fig. 1 shows XRD patterns of the NiO nanospheres prepared by magnetic stirring (a), ultrasound (b) and ultrasound with SDBS surfactant (c). Bragg's peaks at 37.28, 43.23 and 62.78 $2\theta$ were indexed to the (111), (200) and (220) planes of NiO, respectively. All samples have not exhibited the diffraction angles of 30.28 and 50.28 $2\theta$, respectively, indicating not the presence of a $Ni_2O_3$ structure. In the XRD patterns, peak appeared corresponding to (200) and (111) crystal planes of NiO. The NiO-1 prepared under magnetic stirring, the full width at half maximum (FWHM) of XRD peaks decreased indicating that the crystallinity was enhanced and the grain size was increased. On the other hand, a characteristic peak of NiO-3 at $2\theta = 37.28$ is broad indicating a poor crystallinity of the NiO-3. In addition to the difference in the peak width mentioned above, there is also a variation in the relative intensities of the nanosized NiO-1, NiO-2 and NiO-3 XRD diffraction features. The (200) reflection is more intense for nanosized NiO-1 than it is for NiO-2. This intensity variation has previously been observed for NiO particles [16].

For morphologies of the synthesized samples, Fig. 2 shows SEM images of NiO-1 (a), NiO-2 (b) and NiO-3 (c and d) for comparison. It can be seen that surface morphologies of NiO-1, NiO-2 and NiO-3 are different, and the basic shape of NiO-1 is an aggregate of thin flake. Xu et al. [17] reported the flakes to be composed of nanoparticles. Differing from NiO-1, the shape of NiO-2 and NiO-3 is nanospheres and its average sizes are obviously smaller than NiO-1. However, the nanospheres size of NiO-2 is significantly bigger than NiO-3s. Therefore, during synthesis, SDBS plays a crucial role in preventing the random aggregation of nanocrystals and helps to develop the specific morphology. Meher et al. [18] also reported the nickel oxide nanomaterials synthesized using CTAB to be of specific morphology whereas nickel oxide synthesized without CTAB yields no specific morphology. Zheng et al. [19] also investigated the role of CTAB in the development of specific morphology in the synthesis of nickel oxide. The anionic lipids have been used as templates to prepare nanospheres of nickel oxide of 35–75 nm size [20]. This large specific surface area of NiO-3 can provide better electrochemical accessibility to $OH^-$ ions

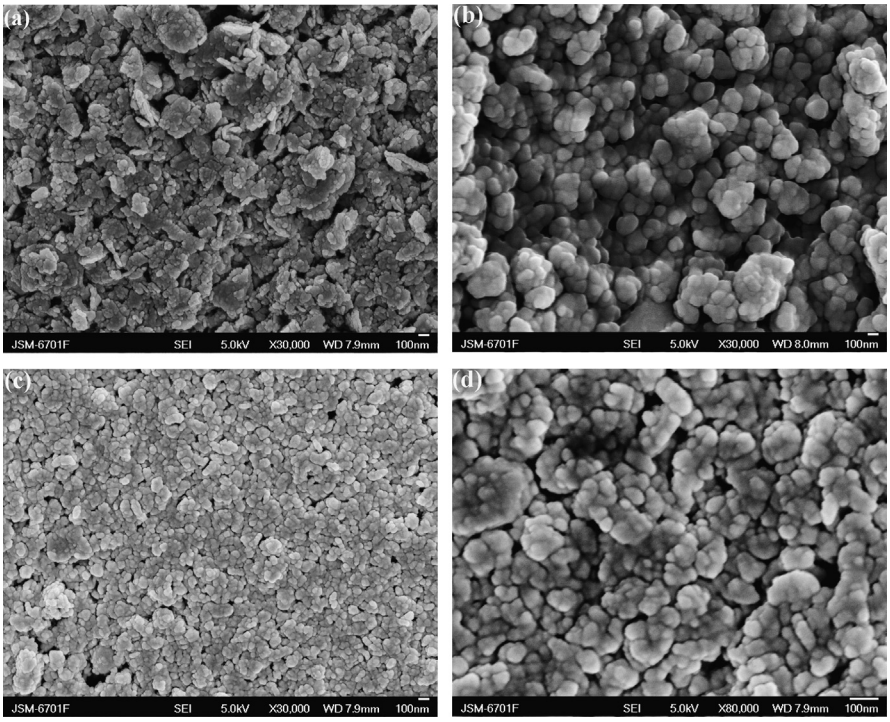


**Fig. 2.** SEM images of the products prepared NiO-1 (a), NiO-2 (b) and NiO-3, (c=30000× and d=80000×).

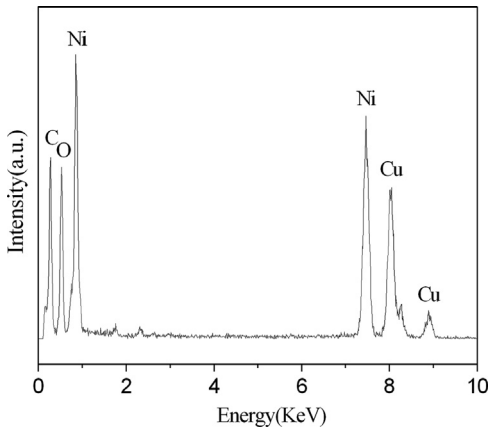


**Fig. 3.** EDX measurement for NiO-3 nanosphere.

into the pores of the active NiO-3 matrix, leading to a high specific capacitance when compared with NiO-1 and NiO-2 samples.

EDX is used to identify the compositions of the composite materials. EDS measurement as shown in Fig. 3 reveals the sample consists of nickel and oxygen besides carbon and cuprum from a C-coated Cu TEM grid. According to the collected data from Fig. 3, it is clear that the as-prepared NiO nanospheres are highly pure.

Fig. 4 shows the TEM images of prepared nickel oxide powder by the ultrasonic method in the presence of SDBS. From these figures, it can observe that the preparation of nickel oxide with SDBS surfactant is the solid spheres with average size 1–3 nm. These values are consistent with those obtained from XRD. The NiO nanospheres controllably as-prepared by the different surfactants show the ionic nature of surfactant has a considerable effect on their morphologies and properties [18,21,24].

Cyclic voltammetry measurements (CV) were employed to investigate the electrochemical behaviors and quantify the specific capacitance of as-prepared NiO electrodes. A NiO capacitor relies on charge storage in the electric double layer at the electrode-electrolyte interface and charge storage in the host material through redox reactions on the surface and hydroxyl ion diffusion in the host material [22]. Fig. 5a shows the CV curves of NiO-1 (a), NiO-2 (b) and NiO-3(c) electrodes recorded in 6.0 M KOH electrolyte at a potential scan rate of 10 mV $s^{-1}$. It is clear that the redox peaks reveal the Faradaic pseudocapacitive property of the NiO based on the surface redox mechanism of $Ni^{2+}$ to $Ni^{3+}$ at the surface of NiO according to the following equation, $NiO+OH^{-}=NiOOH+e^{-}$. From the CV curves, it can be observed that the area under the curves increased in the order NiO-1 < NiO-2 < NiO-3, indicating the highest specific capacitance for the NiO-3 electrode. Fig. 5b shows the CV curves of NiO-3 within potential range of −0.40–0.60 V in 6 M KOH aqueous solution at the scan rate of 5–100 mV $s^{-1}$. The typical Faradaic pseudocapacitive shape of all CV curves in Fig. 5b measured at various scan rates reveals the perfect electrochemical capacitive behavior of NiO-3 electrode [23]. However, with the scan rate increasing, the effective interaction between the ions and the electrode gradually reduced, the deviation from redox peak of the CV becomes obvious.

Charge–discharge cycling tests are performed at a constant current density of 1.0 A $g^{-1}$ with a potential window of −0.2–0.4 V versus Hg/HgO to study the electrochemical

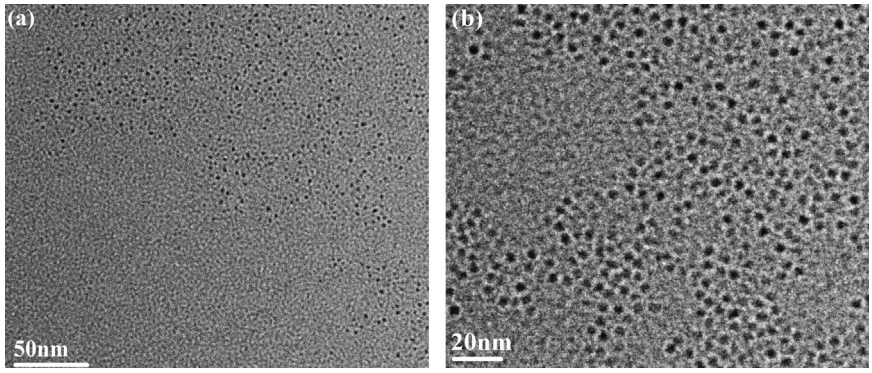


**Fig. 4.** TEM image for prepared NiO-3.

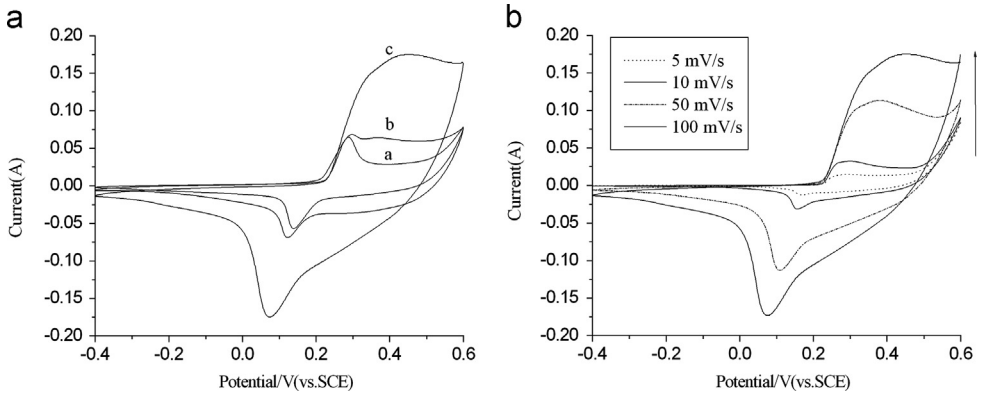


**Fig. 5.** Cyclic voltammetry curves of NiO electrodes within a potential window of −0.4 to 0.6 V versus SCE.

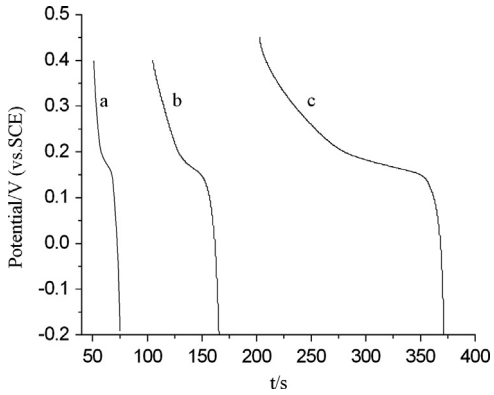


**Fig. 6.** The charge–discharge curve of NiO-1 (a), NiO-2 (b) and NiO-3 (c) at a current density of 1 A $g^{-1}$.

behavior of the synthesized NiO-1 (a), NiO-2 (b) and NiO-3 (c) (Fig. 6). The specific capacitance (SC) is calculated based on the charge–discharge curves using the following equation:

$$SC = \frac{i\Delta t}{\Delta E m} (\mathrm{Fg}^{-1}) \quad (1)$$

where $i$ is the discharge current in amperes, $\Delta t$ is the discharge time in seconds corresponding to the voltage difference ($\Delta E$) in volts excluding iR drop, and $m$ is the mass of the active electrode material in grams. It is observed that there is increment of iR drop through changing the synthesis method as shown in Fig. 6. The obtained values are 46, 107, and 260 F $g^{-1}$ for NiO-1, NiO-2, and NiO-3 electrodes, respectively. The specific capacitance significantly increases with introducing SDBS surfactant under ultrasound conditions. The NiO-3 exhibited higher specific capacitance of 260 F $g^{-1}$ at 1 A $g^{-1}$ current density. This result is consistent with the specific capacitances of the prepared NiO-3 obtained from cyclic voltammograms as shown earlier in Fig. 5b. Besides, it is also observed that the synthesized NiO-3 display discharge slopes which indicate excellent discharge capabilities. Justin et al. [24] investigated the effect of cationic, anionic, and nonionic surfactants for tuning the surface area, pore size, pore volume, and electrochemical properties of NiO powders. The results show the ionic nature of the surfactant has a considerable effect on their capacitance behavior.

The CV curves were used to calculate the specific capacitance of the NiO-3 electrodes at various scan rates. Fig. 7 shows the results of specific capacitance for various scan rates. There is an inverse relation observed between the specific capacitance with scan rates. This is generally caused by insufficient use of the active material involved in the redox reaction under fast scan rates, which may result in a drastic decrease of specific capacitance. However, the reduction of the specific capacitance is not much, by about 32% of the available capacity from 292 to 197 F $g^{-1}$

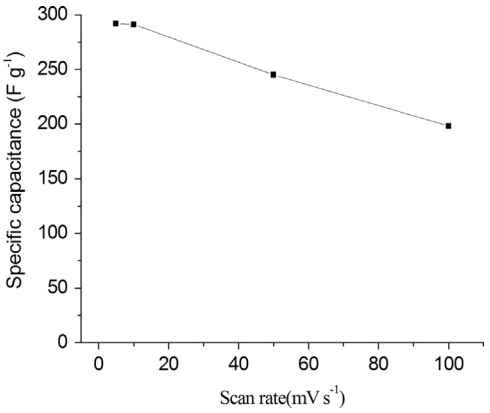


**Fig. 7.** Dependence of the specific capacitance on the scan rates of the NiO-3 electrode.

when the scan rate is increased from 5 to 100 mV $s^{-1}$. It is reasonable to attribute this observation to the size diameter (1–3 nm) and fast surface redox reactivity of the NiO-3 sample exhibiting good power performance.

## 4. Conclusion

NiO nanospheres have been synthesized via the ultrasonic method in the absence or presence of surfactant for the first time. The prepared NiO-3 has average particle size diameter 1–3 nm. Based on the results, the ultrasonic method and SDBS surfactant played the key role in the formation of the nickel oxide nanospheres. However, the introduction of a small amount of SDBS surfactant could obtain smaller nanospheres of the NiO-3 than in the absence of SDBS surfactant. The capacitance of the NiO-3 electrodes was investigated the NiO-3 nanospheres were effective to obtain fully reversible and higher specific capacitance of $\sim$260 F $g^{-1}$ at 1 A $g^{-1}$ current density.

## Acknowledgments

The authors would like to thank funds of Central Universities Fundamental Research (31920130025; 31920130063).

## References

[1] A. Hakim, J. Hossain, K.A. Khan, Renewable Energy 34 (2009) 2625–2629.
[2] M. Matsumiya, F. Qiu, W. Shin, N. Izu, N. Murayama, S. Kanzaki, Thin Solid Films 419 (2002) 213–217.
[3] S.A. El-Safty, Y. Kiyozumi, T. Hanaoka, F. Mizukami, Applied Catalysis A: General 337 (2008) 121–129.
[4] D.H. Prasad, H.I. Ji, H.R. Kim, J.W. Son, B.K. Kim, H.W. Lee, et al., Applied Catalysis B: Environmental 101 (2011) 531–539.
[5] J. Li, F. Meng, S. Suri, W. Ding, F. Huang, N. Wu, Chemical Communications 48 (2012) 8213–8215.
[6] M.M. Rahman, S.L. Chou, C. Zhong, J.Z. Wang, D. Wexler, H.K. Liu, Solid State Ionics 180 (2010) 1646–1651.
[7] A. Ansar, D. Soysal, G. Schiller, International Journal of Energy Research 33 (2009) 1191–1202.
[8] E.O. Zayim, I. Turhan, F.Z. Tepehan, N. Ozer, Solar Energy Materials and Solar Cells 92 (2008) 164–169.
[9] K. Karthik, S.G. Kalai, M. Kanagaraj, S. Arumugam, J. Victor, Journal of Alloys and Compounds 509 (2011) 181–184.
[10] Y. Kobayashi, J. Horiguchi, S. Kobayashi, Y. Yamazaki, K. Omata, D. Nagao, M. Konno, M. Yamada, Applied Catalysis A: General 395 (2011) 129–137.
[11] G. Cravotto, P. Cintas, Chemistry: A European Journal 13 (2007) 1902–1909.
[12] C. Domini, L. Vidal, G. Cravotto, A. Canals, Ultrasonics Sonochemistry 16 (2009) 564–569.
[13] K.S. Suslick, Sonochemistry. Science 247 (1990) 1439–1445.
[14] L.Y. Cao, C. Zhang, J.F. Huang, Materials Letters 59 (2005) 1902–1906.
[15] A. Caballero, L. Hernan, J. Morales, Z. González-Granados, A.J. Sánchez-Herencia, B. Ferrari, Energy Fuels 27 (2013) 5545–5551.
[16] A.C. Gandhi, C.Y. Huang, C.C. Yang, T.S. Chan, C.L. Cheng, Y.R. Ma, S.Y. Wu, Nanoscale Research Letters 6 (2011) 485.
[17] L. Xu, Y.S. Ding, C.H. Chen, L. Zhao, C. Rimkus, R. Joesten, S.L. Suib, Chemistry of Materials 20 (2008) 308–316.
[18] S.K. Meher, P. Justin, G.R. Rao, ACS Applied Materials and Interfaces 3 (2011) 2063–2073.
[19] Y.Z. Zheng, H.Y. Ding, M.L. Zhang, Materials Research Bulletin 44 (2009) 403–407.
[20] K. Sankaranarayanan, V. Hakkim, B.U. Nair, A. Dhathathreyan, Colloids and Surfaces A: Physicochemical and Engineering Aspects 407 (2012) 150–158.
[21] K. Anandan, V. Rajendran, Materials Science in Semiconductor Processing 14 (2011) 43–47.
[22] C.Z. Yuan, X.G. Zhang, L.H. Su, B. Gao, L.F. Shen, Journal of Materials Chemistry 19 (2009) 5772–5777.
[23] S.K. Chang, Z. Zainal, K.B. Tan, N.A. Yusof, W.M.D.W. Yusoff, Current Applied Physics 12 (2012) 1421–1428.
[24] P. Justin, S.K. Meher, G.R. Rao, Journal of Physical Chemistry C 114 (2010) 5203–5210.